Kinetics and Mass Transfer of Benzene Hydrogenation in a Trickle-Bed Reactor

ARTICLE *in* INDUSTRIAL & ENGINEERING CHEMISTRY RESEARCH · SEPTEMBER 2006

Impact Factor: 2.59 · DOI: 10.1021/ie060577a

Kinetics and Mass Transfer of Benzene Hydrogenation in a Trickle-Bed Reactor

Kostas C. Metaxas and Nikos G. Papayannakos*

National Technical University of Athens, School of Chemical Engineering, Heroon Polytechniou 9, Zografos, 157 80 Athens, Greece

Liquid-phase catalytic hydrogenation of benzene was studied in a three-phase bench-scale reactor operating in downflow mode at elevated temperatures and pressures. Reaction kinetics and external gas−liquid mass transfer effects for the system used are estimated. A simplified kinetic expression is used to describe intrinsic kinetics. An analytical model for reactor simulation has been employed incorporating vapor−liquid equilibrium, solvent effects, and mass transfer limitations. Gas- and liquid-side mass transfer coefficients are extracted for the range of the gas and liquid feed flow rates employed in this work. A comparison between the mass transfer values estimated in this work and values from correlations and data reported in the literature is presented. Operation in upflow mode is also compared with downflow mode, and the different reactor performance is discussed.

1. Introduction

1.1. Fixed-Bed Reactors. Trickle-bed reactors (TBRs) are widely used in the chemical industry for various hydrogenation reactions. Operating at elevated temperatures and pressures, they succeed in attaining high conversion per catalyst mass with minimum power consumption, performance that makes them favorable to chemical engineers. Additional aspects regarding TBR advantages and disadvantages as well as operational characteristics are summarized mainly in the reviews of Satterfield,[1] Shah,[2] Herskowitz and Smith,[3] Ramachandran and Chaudhari,[4] Ng and Chu,[5] Gianetto and Specchia,[6] Saroha and Nigam,[7] Al-Dahhan et al.,[8] Dudukovic et al.,[9] and Nigam and Larachi.[10]

In trickle-bed reactors, the gas and liquid phases flow downward through a fixed bed of particles. The upward movement of the two-phase flow is selected for some reactions and applications in order to mainly avoid plugging or temperature runaways. In that case, the reactor is called flooded-bed reactor (FBR). At high gas and liquid superficial mass flow rates, TBRs and FBRs behave alike.[11]

While industrial TBRs are easily simulated by using the pseudo-homogeneous model that incorporates a number of simplifying assumptions, when it comes to micro-, bench-, or pilot-scale laboratory reactors, the complexities associated with transport-kinetic coupling are difficult to incorporate into analytical models. Understanding and quantifying hydrodynamic and mass transfer effects on TBR performance allows the decoupling of transport phenomena and reaction kinetics.

The usual concepts of TBR hydrodynamics include flow regime, pressure drop, liquid holdup, effective catalyst wetting, and liquid flow dispersion. Mass transfer resistances refer to interface transfer and intraparticle diffusion. Pressure drop and liquid holdup, though interrelating with flow regime and wetting efficiency, are out of interest when a small-scale catalytic reactor simulation is attempted.

1.2. Hydrodynamics. 1.2.1. Flow Regime. Three basic flow regimes have been distinguished for TBRs: the trickling flow regime, also known as the low-interaction regime (the liquid phase trickles over the packing in the form of a thin liquid film, while the continuous gas phase moves through the remaining void space, usually cocurrently); the pulsing flow regime (high-interaction regime); and the dispersed bubble-flow regime. Many models (those by Ng[12] and Holub et al.[13]) and flow maps exist mainly for the prediction of regime transition, but the two most significant diagrams depicting flow-pattern boundaries have been published by Fukushima and Kusaka[14,15] and Charpentier.[16] The low gas and liquid Reynolds numbers of this work allow for the assertion of belonging to the trickle-flow regime.

1.2.2. Wetting Efficiency. Regarding the catalyst wetting efficiency, there are numerous studies published. For its estimation, two experimental methods are widely used: the physical "tracer" method[17−19] and the chemical "reaction" method.[20−25] There are also mathematical models that derive analytical solutions of the overall catalyst effectiveness factor in a partially wetted catalyst particle.[26−30] Generally, a large number of variables, such as catalyst bed configuration, pellet features, physical properties of the liquid, and operating conditions, may have an impact on the catalyst wetting.[23]

Dilution of catalyst bed,[17,31,33] elevated pressure—in particular the high gas density,[34,35] and the use of small particles[36] improve catalyst wettability. Llano et al.,[24] working with a slightly bigger particle diameter than that used in this work and investigating the effect of superficial liquid mass velocity—which is the most important factor for accomplishing a fully wetted particle,[21] achieved 100% wetting efficiency in our range of liquid velocities.

1.2.3. Axial Dispersion—Liquid Maldistribution. Small catalyst beds and low liquid flow rates are the main reasons of extended axial dispersion effects on reactor performance.[2,37] The use of fine catalyst particles or the bed dilution with inert fine particles prevents such phenomena as radial or axial dispersion to influence reactor performance,[32,38] and in combination with high gas and liquid flow rates before every single experiment—operation in the high-interaction regime before each experiment but without soaking the bed overnight[35], the absence of liquid maldistribution is ensured.

1.3. Mass Transfer. 1.3.1. Intraparticle Mass Transfer. Mass transfer limitations originating from the diffusion of the reactants into the pores of the catalyst can be neglected when small catalyst particles are used. The internal surface of the catalyst is fully wetted as pores are completely filled with liquid because of capillary forces.[39]

1.3.2. Interface Mass Transfer Correlations. Interparticle mass transfer phenomena regarding gas−liquid transportation

* Corresponding author. E-mail: npap@central.ntua.gr. Tel.: +30 210 772 3239. Fax: +30 210 772 3155.

10.1021/ie060577a CCC: $33.50
Published on Web 09/16/2006

in trickle-bed reactors have been examined in a wide range of operating conditions. Shah[2] and Turek and Lange[40] reviewed the most widely used correlations for the estimation of mass transfer coefficients, while Morsi et al.,[41] Yaichi et al.,[42] and Wild et al.[43] proposed new ones. Iliuta et al.[44] compiled over 3200 experimental data, and by combining dimensional analysis with artificial intelligence (neural networks), they derived state-of-the-art correlations on a large variety of fluid physical properties, operating conditions, and geometrical properties of packing, column, and particle shape. This group of researchers has also given the most recent publication[45] on gas−liquid mass transfer in packed beds.

1.3.3. Experimental Estimation of Mass Transfer. Goto and Smith,[46] Martin et al.,[47] Turek and Lange,[40] and Samb et al.[48] are among the few that have investigated gas−liquid mass transfer by physical methods at low liquid flow rates. Only recently have researchers worked on the effect of pressure on gas−liquid mass transfer.[34,49,50] Wammes et al.[34] concluded that elevated gas densities increase only interfacial areas. Larachi et al.[50] presented a comprehensive database of previous studies regarding the effect of pressure on mass transfer parameters, proposing a phenomenological description in accordance with a semiempirical two-zone model for the evaluation of the volumetric liquid-side mass transfer coefficients.

Midoux et al.[51] determined mass transfer parameters by chemical technique using organic liquids. Goenaga et al.[52] used dynamic methods to study gas-to-liquid mass transfer in trickle-bed reactors, indicating a strong dependence of mass transfer coefficient on gas flow rate, while Toppinen et al.[53] modeled mass transfer using both Stefan−Maxwell equations and the effective diffusivity method, extracting similar results. Iliuta and Thyrion[54] showed that, in the trickle-flow regime, volumetric liquid mass transfer coefficients obtained by physical and chemical absorption are close and axial dispersion is significant at low liquid velocities and high initial concentration of the liquid reactant.

Sparse data exist in the literature on the mass transfer characteristics of a fixed bed with cocurrent upflow.[37,47,49] The values of the liquid-side mass transfer coefficients of Lara Marquez et al.[49] are 1 order of magnitude lower than those of Stuber et al.,[37] although the latter worked at lower liquid flow rates.

Evren and Özdural[55] developed a new technique to calculate liquid film mass transfer coefficients, and Benadda et al.[56] determined volumetric liquid-side mass transfer coefficients during gas−liquid absorption in a countercurrent packed-bed column. Bin et al.[57] estimated ozone mass transfer coefficients in a tall bubble column, while Dluska et al.[58] measured mass transfer coefficients for the physical and chemical absorption in a gas−liquid Couette−Taylor flow reactor.

However, mass transfer data at low gas and liquid flow rates such as those prevailing for benzene hydrogenation in small bench-scale reactors do not exist. Therefore, multiphase models describing the composition change of reactants and products in both liquid and gas phases along the reactor length cannot be developed for the simulation of this system.

1.4. Reaction Kinetics. 1.4.1. Gas- and Liquid-Phase Kinetics. There are few journal publications that concern benzene hydrogenation in a trickle-bed reactor.[11,59,60] Only that of Sharma et al.[60] considers the reaction kinetics of benzene hydrogenation to cyclohexane in a trickle-bed reactor, not on a Ni/Al_2O_3 catalyst yet.

In contrast to the gas-phase reaction, which is widely studied by various researchers as a model aromatic hydrogenation reaction over group VIII metal catalysts [Chou and Vannice,[61] Zrncevic and Rusic[62] (review of kinetic models), Coughlan and Keane,[63] Lin and Vannice,[64] Stanislaus and Cooper[65] (extended review on aromatic hydrogenation), Smeds et al.[66] (ethylbenzene), Keane and Patterson,[67] Louloudi et al.,[68] and Saeys et al.[69]], kinetic analysis of liquid-phase benzene hydrogenation is rarely reported in the literature [Murzin et al.,[70] Toppinen et al.,[71] Singh and Vannice,[72] and Franco et al.[73]]. However, even in the foresaid publications, the reaction takes place in a batch [Franco et al.[73]], semibatch [Singh and Vannice,[72] Toppinen et al.[71]], or shacked [Murzin et al.[70]] reactor with various commercial or laboratory-produced catalysts (Pt [Franco et al.[73]], Pd [Singh and Vannice[72]], and Ni [Murzin et al.,[70] Toppinen et al.[71]]).

A number of interesting features of liquid-phase hydrogenation can be found in the dissertations of Rautanen (http://lib.tkk.fi/Diss/2002/isbn9512262096/isbn9512262096.pdf) and Lylykangas (http://lib.tkk.fi/Diss/2004/isbn9512269139/isbn9512269139.pdf), whose main difference from this work is that they regard the kinetic modeling of toluene and not benzene—although both monoaromatics—in a continuous stirred tank reactor. Rantakylä et al.[74] hydrogenated toluene as well, in a laboratory-scale trickle-bed reactor similar to the one used for benzene hydrogenation in this work.

Murzin and Kul'kova[75] examined thoroughly benzene hydrogenation on different metal catalysts. They proposed a reaction mechanism based on the formation of cyclohexene on the catalyst surface,[70] from which they derived the kinetic expression of the reaction. Franco et al.[73] suggested four mechanisms assuming Langmuir−Hinshelwood−Hougen−Watson (LHHW), competitive or noncompetitive, and dissociative or nondissociative adsorption for benzene and hydrogen. In this way, they extracted eight different kinetic models, with the one standing for nondissociative noncompetitive adsorption of both reactants being the most promising. Both researchers used partial pressure of hydrogen in the kinetic expressions.

1.4.2. Solvent Effect. Singh and Vannice[72] and Rautanen et al.[76] marked the magnitude of the solvent effect on the final result and proposed the use of liquid-phase hydrogen concentration instead of hydrogen partial pressure in the kinetic rate. Toppinen et al.[71] used also hydrogen concentration in the rate expression. They fitted two mechanistic models to the experimental data, including that of Murzin et al.,[70] which proved insufficient to describe the data well. The qualified model was one based on competitive adsorption of hydrogen and the aromatic compound.

1.4.3. Activation Energy. Apparent activation energies for gas-phase benzene hydrogenation on Ni vary in the range 26−94 kJ/mol[63] with the large majority lying between 28 and 58 kJ/mol. Singh and Vannice[72] and Toppinen et al.,[71] working on Pd/Al_2O_3 and Ni/Al_2O_3, respectively, calculated exactly the same apparent activation energy (37.7 kJ/mol). Chou and Vannice[61] measured an apparent activation energy of ∼53 kJ/mol for gas-phase hydrogenation of benzene on supported and unsupported Pd catalysts, and Murzin et al.[70] calculated E_a equal to 41.5 kJ/mol for liquid-phase hydrogenation. From liquid-phase benzene hydrogenation studies on Pt, Franco et al.[73] gave an apparent activation energy value of 35.4 kJ/mol, while Lin and Vannice[64] and Saeys et al.,[69] by conducting gas-phase hydrogenation of benzene, found values of 42−54 and 104 kJ/mol, correspondingly. The value of apparent activation energy published from Murzin et al.[70] for liquid-phase benzene hydrogenation on Ni/C is 61.5 kJ/mol. Two gas-phase reaction studies—on Ni−Y zeolite and Ni/SiO_2—by Coughlan and Keane[63] and Keane and Patterson[67] reported values of apparent

activation energies of 59.5 and 29.1 kJ/mol, respectively. Louloudi et al.[68] reported activation energies between 42 and 53 kJ/mol for benzene hydrogenation on *x*NiATOS catalysts. From the above notes, it is easily concluded that the activation energy varies in a wide range depending on the catalyst used and the experimental system employed in each work.

1.5. Scope of the Paper. The scope of this paper is to study reaction kinetics and mass transfer characteristics of benzene hydrogenation over a commercial catalyst in a bench-scale trickle-bed reactor. To this end, the fitting of the rival kinetic models to experimental data is discussed, the best one for simulation purposes is proposed, and the interfacial gas−liquid mass transfer coefficients for this system are estimated and compared with literature data. A comparison of upflow with downflow three-phase reactor performance is also presented.

2. Experimental Section

The liquid-phase hydrogenation of benzene took place in an integral, isothermal, laboratory bench-scale trickle-bed reactor. The inner diameter of the reactor tube is 1 in., and its total length is 47.5 cm. The temperature of the catalyst bed was monitored and controlled via five thermocouples placed inside a thermowell with an external diameter of 4 mm. The control of the temperature within ±1 °C is accomplished by software proportional−integral−derivative (PID) controllers, which, through a system of solid-state relays, supply with the appropriate energy every single of the four resistors that "embrace" the reactor.

A piston-bearing pump drives liquid downward or upward depending on the preferred mode of operation. The whole unit resembles commercial ones, as it is semiautomated with the operating parameters being controlled from a main personal computer equipped with a data acquisition card to digitalize analogue signals, which have been collected and intensified by a multiplexer card. User-friendly software allows the easy handling of the signals for either their surveillance or control.

The liquid product of the reaction is collected and analyzed with the help of a gas chromatographer. Repeatability of GC analysis was estimated to be ±3%. The concentration of *n*-hexane, benzene, and cyclohexane in the samples is determined, while toluene is used as an internal calibrator.

The experiments were conducted at temperatures in the range of 70−100 °C and total pressure of 16 bar. The minimum mass liquid flow rate was 59 g/h and the maximum was 170 g/h, corresponding to weighted hourly space velocities of 20−60 h^{-1}. The gas flow rate changes between 1.4 and 31.4 NL/h. The concentration of benzene in the liquid feed was varied from 1.45 to 7 wt %. *n*-Hexane was used as the solvent together with cyclohexane (0−27.3 wt %).

The catalyst comes from commercial Ni/Al_2O_3 extrudates that were crushed, and the particles used in this study were collected between sieves with openings of 0.315 and 0.4 mm. The diluted catalytic bed was 7 cm long and consisted of 3 g of catalyst and 50 g of inert carborundum (SiC) particles with a mean diameter of 0.25 mm. Before and after the catalyst bed, two impeded zones, one from glass spheres of 3 mm in diameter and another of 4 mm, secure uniform liquid distribution and support the catalyst bed. The loading of the bed is dense as portions of catalyst and diluent carborundum were sequentially added in the continuously shaken reactor.

After activating the catalyst, stabilization was attempted for 50 h at 100 °C. Deactivation was followed by repetition of standard experiments. During the first circle of experiments, a smooth deactivation of the catalyst with time was observed and has been taken into account. In the beginning of each experiment, high liquid and gas flow rates were used to wet catalyst and avoid liquid maldistribution. The steady state of an experiment was achieved after 6−10 h of continuous operation depending on liquid and gas flow rates.

3. Kinetic Expressions

A number of kinetic equations have been published in the literature for benzene hydrogenation, and the most appropriate for this work are summarized in the following. Franco et al.[73] suggested the following four kinetic expressions for benzene hydrogenation, with the first being qualified:

$$r_p = \frac{kK_H K_B C_B P_H}{(1 + K_H P_H)(1 + K_B C_B + K_C C_C)} \tag{1}$$

$$r_p = \frac{kK_B C_B \sqrt{K_H P_H}}{(1 + \sqrt{K_H P_H})(1 + K_B C_B + K_p C_p)} \tag{2}$$

$$r_p = \frac{kK_H K_B C_B P_H}{(1 + K_H P_H + K_B C_B + K_p C_p)^2} \tag{3}$$

$$r_p = \frac{kK_H K_B C_B P_H}{(1 + \sqrt{K_H P_H} + K_B C_B + K_p C_p)^3} \tag{4}$$

Toppinen et al.[71] tried two kinetic models (eq 5 = simplified Murzin et al.[70] and eq 6 = simplified Smeds et al.[66]), where $\gamma = 1$ for molecular adsorption or $\gamma = 2$ for dissociative adsorption.

$$r_p = \frac{kC_B C_H}{\frac{k}{k_3} C_H C_B + \frac{1}{K_4} C_C + C_B} \tag{5}$$

$$r_p = \frac{kK_H K_B C_B C_H}{[3K_B C_B + (K_H C_H)^{1/\gamma} + 1]^{\gamma+1}} \tag{6}$$

Murzin et al.[70] proposed the following kinetic equation:

$$r_p = \frac{kN_B P_H}{N_B + k''(1 - N_B) + k' N_B P_H} \tag{7}$$

The study by Singh and Vannice[72] resulted in the following kinetic form:

$$r_p = \frac{kK_H K_B C_B C_H}{(1 + \sqrt{K_H C_H})(\sqrt{K_H C_H} + K_B C_B \sqrt{K_H C_H} + K_D K_B C_B)} \tag{8}$$

From the above kinetic expressions, the ones that best fitted our data are eq 1 (Model 1) using hydrogen concentration in the liquid phase instead of hydrogen partial pressure in the gas phase and neglecting the cyclohexane term, as well as eq 6 with $\gamma = 2$ (Model 2). Moreover, a classical LHHW kinetic form (eq 9, Model 3) and the simpler eq 10 (Model 4) have been proved to fit very well our experimental data.

$$r_p = \frac{kC_B C_H}{(1 + K_H C_H + K_B C_B)^2} \tag{9}$$

$$r_p = \frac{kC_B C_H}{1 + K_H C_H + K_B C_B} \tag{10}$$

Cyclohexane concentration is not used as an inhibiting factor because its weak influence on conversion was experimentally verified for the catalyst used in this work.

4. Simulation Model

Two forms of kinetic models can be incorporated into reactor simulation codes: a pseudo-homogeneous form and a heterogeneous one. Although pseudo-homogeneous models have been widely used for the simulation of industrial trickle-bed reactors, the development of more detailed models is inevitable, especially in scale-up/down studies and in catalyst and kinetic research. Preliminary tests conducted with the use of a pseudo-homogeneous model depicted its clear weakness in fitting our experimental results. Therefore, a model incorporating volatilization effects and gas−liquid mass transfer resistance was developed in an attempt to better outline reality in the catalyst bed reactor.

The basic parts of the simulation model consist of the first-order ordinary differential equations corresponding to mass balances and the nonlinear unconstrained optimization technique[77] for the data fitting. The fourth-order Runge−Kutta[78] method was used for the arithmetic solution of the differential equations, while the modified Levenberg−Marquardt method (Visual Numerics: IMSL Math/Library) was selected for the optimization.

The volatility of the liquid reactants was taken into account by utilizing Soave−Redlich−Kwong cubic equation of states[79] and estimating the vapor−liquid equilibrium constants with the Newton−Raphson method. Gas−liquid equilibrium was assumed at the reactor inlet.

In the following mass balances of the simulation model for the gas and liquid phases, gas−liquid mass transfer resistances have been considered, while in the kinetic expressions, the concentrations of the reactants in the liquid phase are used. Mass transfer rates are calculated on the basis of the thin-film theory.

In the liquid phase, the differential mass balances for the reactants along the reactor axis are

$$\frac{dN_{LB}}{dz} = aN_{GLB} - r_p\rho_{bed}A = \left[k_{GLB}a\left(\frac{P_B}{H_B} - C_{LB}\right) - r_p\rho_{bed}\right]A \tag{11}$$

$$\frac{dN_{LH}}{dz} = aN_{GLH} - 3r_p\rho_{bed}A = \left[k_{GLH}a\left(\frac{P_H}{H_H} - C_{LH}\right) - 3r_p\rho_{bed}\right]A \tag{12}$$

and the corresponding ones for the gas phase are

$$\frac{dN_{VB}}{dz} = k_{GLB}a\left(\frac{P_B}{H_B} - C_{LB}\right)A \tag{13}$$

$$\frac{dN_{VH}}{dz} = k_{GLH}a\left(\frac{P_H}{H_H} - C_{LH}\right)A \tag{14}$$

Equilibrium at the gas−liquid interface can be described by

$$P_i^* = H_iC_{iL}^* = C_{iG}^*RT \tag{15}$$

$$C_{iG}^* = C_{iL}^*(H_i/RT) = C_{iL}^*H_i^* \tag{16}$$

while the gas-side and liquid-side mass transfer coefficients are correlated as

$$k_{GLi} = \frac{1}{\frac{1}{k_{Li}} + \frac{1}{k_{Gi}H_i^*}} = \frac{1}{\frac{1}{k_{Li}} + \frac{RT}{k_{Gi}H_i}} \tag{17}$$

The gas- and liquid-side mass transfer coefficients are related to the corresponding film thicknesses (l) and diffusion coefficients (D_{Gi} or D_{Li}) by the following relations:

$$k_{Li} = \frac{D_{Li}}{l} \Rightarrow a_vk_{Li} = D_{Li}\frac{a_v}{l} \Rightarrow \frac{a_v}{l} = \frac{a_vk_{Li}}{D_{Li}} \tag{18}$$

$$k_{Gi} = \frac{D_{Gi}}{l} \Rightarrow a_vk_{Gi} = D_{Gi}\frac{a_v}{l} \Rightarrow \frac{a_v}{l} = \frac{a_vk_{Gi}}{D_{Gi}} \tag{19}$$

For the estimation of the kinetic parameters, which are strongly correlated with each other, a reparameterization technique—reduction of interaction of parameters by appropriate transformation—has been applied.[80] This reparameterization method allows initial values from an extended range to be tested, ensuring the avoidance of local minima.[81]

Eight parameters are to be estimated: θ and φ for the three kinetic constants and overall mass transfer coefficients ak_{GL} of benzene and hydrogen for every single experiment. To overcome the drawback of the large number of parameters, we have selected a set of 23 experiments that have similar gas- and liquid-phase velocities. Then, this set is used for the estimation of the kinetic constants as well as the values of the overall mass transfer coefficients for benzene and hydrogen that are the same for all the experiments of the set as the hydrodynamics of the gas−liquid interface is similar. Assuming thermodynamic equilibrium at the catalyst bed inlet, the concentration profiles in the gas and liquid phases along the bed are calculated by solving the mass balance eqs 11−14.

All the effort is focalized on the minimization of the objective function Φ that incorporates the experimental and parameters' estimation errors and is expressed as the sum of the squared differences of experimental and calculated benzene conversion percent at the reactor exit for the 23 experiments.

$$\Phi_{min} = \sum_{i=1}^{N_{exp}}(X_i - \hat{X}_i)^2 \tag{20}$$

5. Results

5.1. Reaction Kinetics. By minimizing eq 20 for the four rival models, as discussed before, the values given in Table 1 were obtained for preexponential factors, apparent activation energies, adsorption enthalpies, and overall mass transfer coefficients for hydrogen and benzene. The similarity of the values estimated for the overall mass transfer coefficients for benzene and hydrogen using any of the four models indicates that these parameters are reliably estimated.

As already mentioned, the apparent activation energy of benzene hydrogenation stands in the range of 26−94 kJ/mol, which is in good agreement with the values predicted in this work for all models. The adsorption enthalpy of benzene is expected to be much higher than that predicted for Models 1 and 2, in the range of 40−60 kJ/mol at medium coverage[66] or 50−105 kJ/mol at monolayer coverage according to Keane and Patterson[67] on nickel metal. Hydrogen adsorption enthalpy usually lies between 30 and 42 kJ/mol[61] and 40−120 kJ/mol (calorimetric and TPD studies),[66] while Lindfords et al.[82] reported an adsorption enthalpy of 104 kJ/mol for liquid-phase

Table 1. Preexponential Factor, Activation Energy, Adsorption Enthalpy of Benzene and Hydrogen, Overall Gas−Liquid Mass Transfer Coefficients for Benzene and Hydrogen, and Objective Function for the Four Qualified Kinetic Models

models	1	2	3	4
A_1	1.24E+14	8.31E+13	3.81E+12	4.95E+13
E_a (J/mol)	4.87E+04	4.77E+04	3.87E+04	4.78E+04
A_2	5.53E−03	1.77E−09	1.53E−04	1.49E−36
ΔH_{H_2} (J/mol)	4.29E+04	7.99E+04	5.14E+04	2.60E+05
A_3	1.93E+03	3.95E+02	2.61E+01	2.63E+00
ΔH_B (J/mol)	5.72E+03	5.70E+03	1.56E+04	2.50E+04
ak_{GLH_2} (s^{-1})	2.90E−02	2.97E−02	3.20E−02	4.18E−02
ak_{GLB} (s^{-1})	1.47E−05	1.72−05	1.80E−05	1.75E−05
$\sqrt{\Phi_{min}/N_{exp}}$	1.1987	1.2231	1.2320	1.2308

toluene hydrogenation on Ni/Al_2O_3. All models tested except Model 4 give reasonable values for hydrogen adsorption enthalpy.

However, all models fit very well the experimental data as indicated by the values of Φ_{min}/N_{exp} in Table 1 and observed in Figure 1. Model 1 generates the minimum deviation between predicted and experimental values of benzene conversion, and this is used in the following, for the estimation of the mass transfer coefficients of every single experiment.

5.2. Mass Transfer Effects. The effect of the gas velocity on reactor operation was studied by changing the gas flow rates, while the range of the liquid flow rate was narrow and the change of the liquid velocity is not expected to considerably affect the mass transfer coefficients. Eighty-eight experiments were conducted in the temperature range in which the reaction kinetics was estimated, namely, 70−100 °C. Seventy-nine experiments took place in downflow mode and nine took place in upflow mode, for the sake of comparison.

The overall mass transfer coefficients of benzene and hydrogen for every single experiment were first estimated. By processing the experimental data, it was made clear that the change of the benzene overall mass transfer coefficient had little effect on the results. Particularly for values $<10^{-3}$ s^{-1}, a 1000-fold variation of the coefficient altered the result by 5% at most. For values $>10^{-3}$ s^{-1}, the equilibrium was reached, and so there was no benzene transfer between the gas and liquid phases. Therefore, hydrogen gas−liquid mass transfer mainly affects the reactor performance, while benzene mass transfer is of minor importance.

Equilibrium calculations yield that >95% of the total benzene is present in the liquid phase, and even if no benzene was transferred from the gas phase to the liquid phase, that present in the liquid-phase benzene at the entrance would be sufficient in most cases for the conversions we measured, <95%. On the opposite side, that diluted in the liquid-phase hydrogen was <10% of that needed for the conversions measured, while its concentration in the gas phase was dropping up to 60% along the reactor length. This implies that hydrogen mass transfer effects predominate at the conditions in which the reaction was studied.

Figure 2 presents the values of ak_{GL} for hydrogen versus the average—along the reactor's catalytic bed—superficial velocity of the gas phase for the downflow and upflow experiments. From this figure, it is observed that the overall gas−liquid mass transfer coefficient for hydrogen transport strongly depends on gas velocity in both upflow and downflow experiments. Moreover, for superficial gas velocities <0.1 cm/s, the upflow mass transfer coefficient is distinctly less than the corresponding downflow one, while the difference between the two values diminishes as the velocity increases.

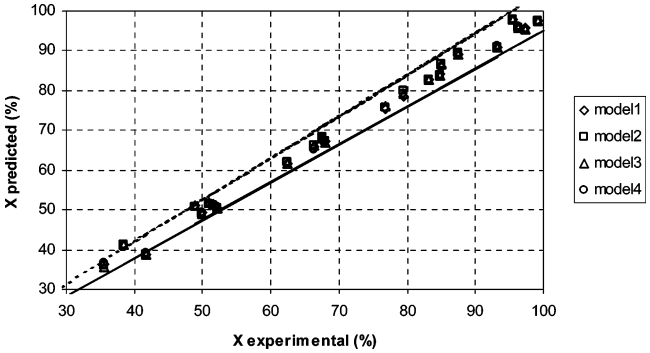

Figure 1. Parity plot of experimental versus predicted benzene conversions for the four qualified kinetic models (lines present ±5% confidence zones).

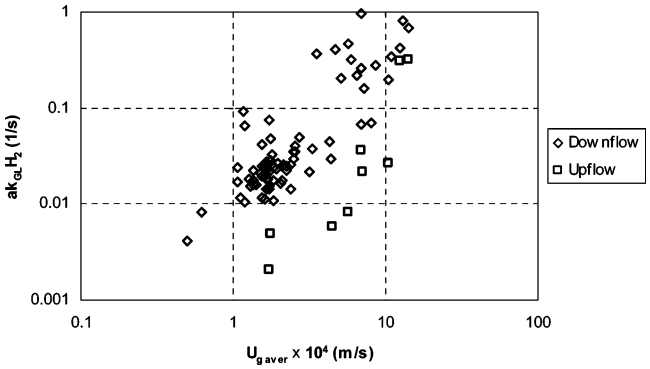

Figure 2. Overall mass transfer coefficient of hydrogen versus average superficial gas velocity for downflow and upflow modes of operation.

The effect of the gas-phase superficial velocity on the gas-side and liquid-side mass transfer coefficients is considerable and is always taken into account in the various correlations proposed in the literature.[40,45] Thus, the dependence of the gas- and liquid-side mass transfer coefficients on the gas superficial velocity has been investigated using the available experimental data. This was attempted by associating the ratio a/l ($= ak_{Gi\text{ or }Li}/D_{Gi\text{ or }Li}$) on the gas and liquid sides, with the average superficial velocity of the gas phase through an exponential relationship. This form of dependence is widely used in the literature—although sometimes power equations incorporating Reynolds number instead of gas velocity are preferred (Table 2)—and it is observed from Figure 2 to hold for the overall mass transfer coefficient. In this way, we obtained the following two equations for the trickle-flow operation:

$$\ln(ak_{Li}/D_{Li}) = \ln(a/l) = 1.17\ln(U_{g\,aver}) + 9.32 \quad (21)$$

$$\ln(ak_{Gi}/D_{Gi}) = \ln(a/l) = 2.52\ln(U_{g\,aver}) + 9.40 \quad (22)$$

Figure 3 presents the parity plot of the benzene conversions measured for the downflow experiments. The predictions are fairly good, with ~10 out of 79 experimental points falling out of the deviation limit of 10% between predicted and experimental values for benzene conversion.

In Figure 4, the estimated gas- and liquid-side mass transfer coefficients are presented. It is observed that the hydrogen gas-side mass transfer coefficients are 1 order of magnitude higher than the corresponding coefficients for benzene mass transfer, while the liquid-side hydrogen mass transfer coefficients have ~5× larger values than the benzene ones. The velocity impact on the mass transfer coefficients appears to be more extended for the gas-side transport than for the liquid-side transport.

The overall mass transfer coefficients for hydrogen and benzene that result from relations 21 and 22 are presented in

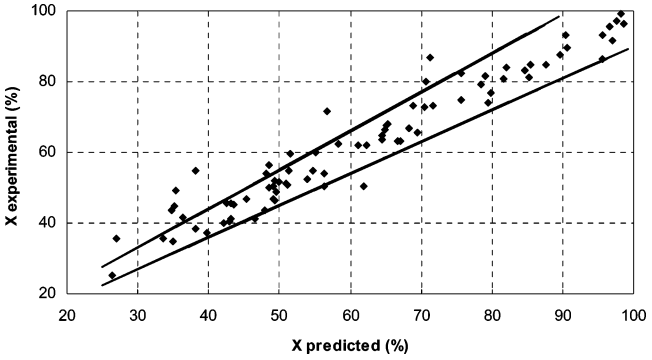

Figure 3. Parity plot of experimental versus predicted conversions of benzene extracted from optimization for estimating mass transfer coefficients (continuous lines present ±10% deviation zones).

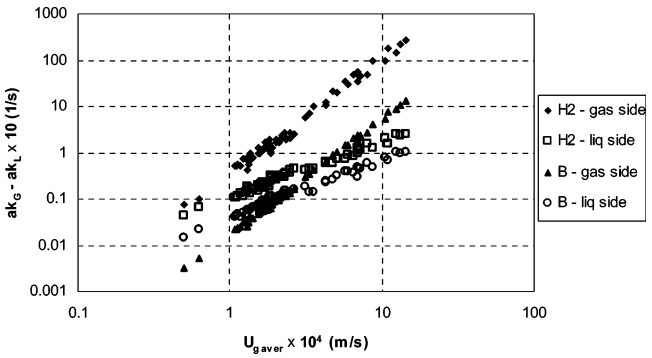

Figure 4. Gas- and liquid-side mass transfer coefficients for benzene (B) and hydrogen (H2) versus average superficial gas-phase velocity for downflow.

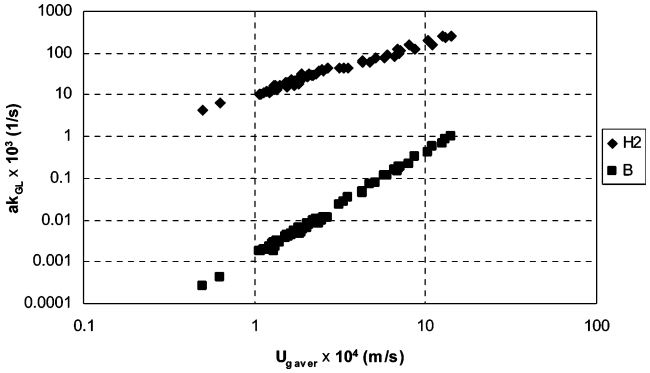

Figure 5. Overall mass transfer coefficients for benzene (B) and hydrogen (H2) versus average superficial gas-phase velocity for downflow.

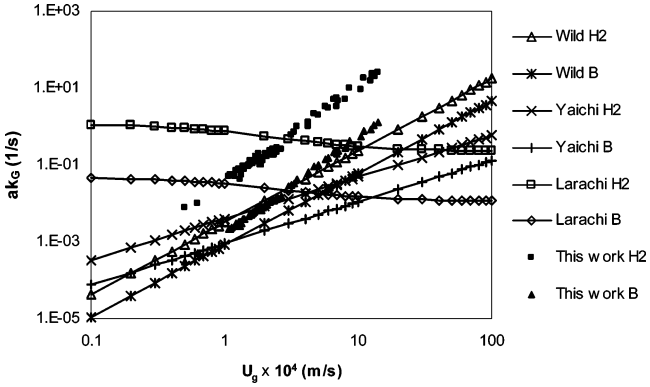

Figure 6. Comparison of our results of gas-side mass transfer coefficient with predictions of literature correlations for hydrogen (H2) and benzene (B).

Figure 5. Although the predicted values for hydrogen transfer are less scattered compared to those of Figure 2, the range in which they vary is about the same. Moreover, it is observed that the overall mass transfer coefficient for the benzene transfer is very low compared to that of hydrogen; however, this does not affect the process because of the practically negligible amounts of benzene demanded to be transferred from the gas phase to the liquid phase, as discussed before.

Turek and Lange[40] (eq 24, Table 2), Midoux et al.,[51] and Morsi et al.[41] report liquid-side mass transfer correlations for gas−liquid systems flowing through fixed beds. In these works, the form of eq 23 (Table 2) first published by Goto and Smith[46] is used. Ellman et al.[83] proposed a more complicated algebraic equation (eq 25, Table 2), which is also used by Gianetto and Specchia.[6] Wild et al.[43] published also some mass transfer correlations based on eq 26, distinguishing between low-, high-, and transition-interaction regimes. Iliuta et al.[44] started using neural networks instead of algebraic equations, and Larachi et al.[45] improved and expanded to heat transfer this kind of correlation. While many correlations exist for the liquid-side mass transfer, only a few have been published for the gas-side mass transfer. Those published from Yaichi et al.[42] (eq 28, Table 2) and Wild et al.[43] (eq 27, Table 2) are presented together in the paper by Iliuta et al.[44] Finally, Larachi et al.[45] gave a complete set of equations for predicting mass transfer correlations.

In Figures 6 and 7, a comparison of our results with literature data is attempted. For the accomplishment of this comparison, a number of physicochemical properties need to be used. As our experiments were performed at a relatively narrow range

Table 2. Mass Transfer Correlations Published in Literature

authors	correlations	
Goto−Smith[46]	$ak_{L(G-S)} = 4440 D_l (Re_l^{0.4})(Sc_l^{0.5})$	(23)
Turek−Lange[40]	$ak_{L(T-L)} = 16.8 D_l (Ga^{-0.22})(Re_l^{0.25})(Sc_l^{0.5})$	(24)
Ellman et al.[83]	$ak_{L(Ell)} = 0.45\left(\frac{D_l}{d_K^2}\right)(X_G^{0.65})(Re_l^{1.04})(We_l^{0.26})(Sc_l^{0.65})\left(\frac{a_s d_K}{(1-\epsilon)}\right)^{0.325}$	(25)
Wild et al.[43]	$ak_{L(W)} = (2.8\times10^{-4})\left(\frac{D_l}{d_K^2}\right)\left[(X_G^{0.25})(Re_l^{0.2})(We_l^{0.2})(Sc_l^{0.5})\left(\frac{a_s d_K}{(1-\epsilon)}\right)^{0.25}\right]^{3.4}$	(26)
Wild et al.[43]	$ak_{G(W)} = 0.067\left(\frac{D_g}{d_K^2}\right)\left[(X_G^{0.5})(Re_g^{0.8})(We_g^{0.2})(Sc_g^{0.5})\left(\frac{a_s d_K}{(1-\epsilon)}\right)^{0.25}\right]^{1.1}$	(27)
Yaichi et al.[42]	$ak_{G(Y)} = 0.049 D_g\left(\frac{a_s}{d_p}\right)^{0.985}(Re_g^{1.08})(Re_l^{0.2})(Sc_g^{0.5})\left(\frac{d_p}{d_c}\right)^{0.72}$	(28)

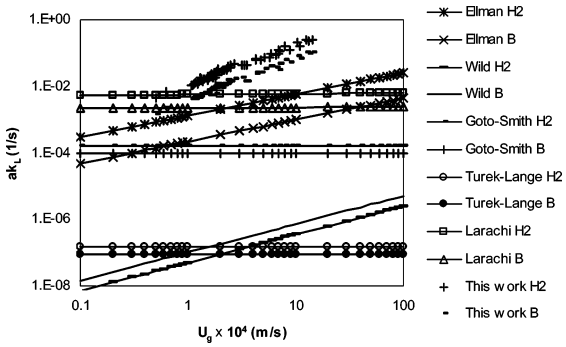

Figure 7. Comparison of our results of liquid-side mass transfer coefficient with predictions of literature correlations for hydrogen (H2) and benzene (B).

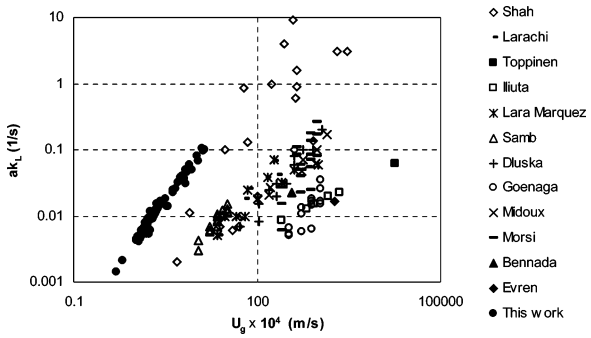

Figure 8. Comparison of our results of liquid-side mass transfer coefficient for benzene with published experimental data of various systems.

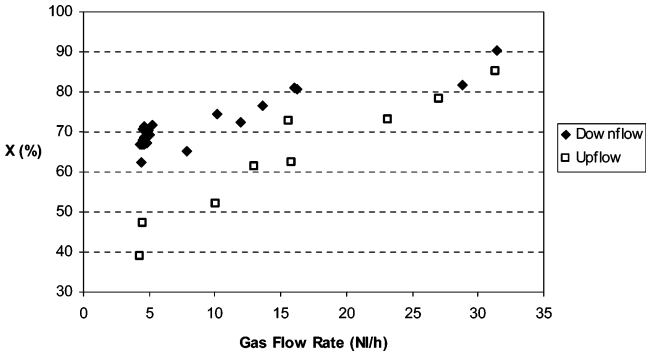

Figure 9. Benzene conversion versus gas flow rate for upflow and downflow operation.

of liquid velocities for which the velocity changes are not expected to have a remarkable impact on mass transfer coefficient values, an average value for liquid velocity is used in all calculations and comparison figures.

In Figure 6, the predicted values from the equations given in Table 2 for the gas-side mass transfer coefficient are plotted along with the curves derived from a recent publication correlating operating conditions with mass transfer through a neural network method.[45] The neural network of the latter work has been developed with data for gas velocities between 0.38 and 200 cm/s and liquid velocities from 0.045 to 1.62 cm/s, and the curve in our drawing is an extrapolation. Although the gas velocities of this work are lower than those used from the previous investigators, the estimated gas-side mass transfer coefficients are not far from their predictions. The correlations proposed by Yaichi et al.[42] and Wild et al.[43] (eqs 27 and 28, Table 2) predict lower values than those estimated in this study, while predictions by Larachi et al.[45] seem unaffected by gas velocity and exhibit higher values than this work at low gas velocities ($<3 \times 10^{-2}$ cm/s) and lower values at high velocities.

In Figure 7, the liquid-side mass transfer correlations estimated in this work and calculated from literature correlations are presented. Liquid and gas velocity ranges used by Turek and Lange[40] and Larachi et al.[45] are closer to the ones used in this work. Ellman et al.[83] reported that their correlation is reliable for $10^{-6} < X_G < 0.8$, when X_G values of this work stand between 0.08 and 2.

Most of the correlations connect liquid-side mass transfer coefficients only with liquid velocity and gas-side mass transfer coefficients only with gas velocity. Larachi et al.[45] take into account both velocities for estimating gas- and liquid-side mass transfer coefficients. Nevertheless, Figure 7 includes all correlations independent of what liquid velocities were used for their derivation. In general, these correlations may not be appropriate for such low gas and liquid superficial velocities as those we have worked with. Correlations given by Ellman et al.[83] and Larachi et al.[45] predict liquid-side mass transfer coefficient data (ak_L) close to those estimated in this work, while the rest of the correlations predict lower values by more than an order of magnitude.

Furthermore, sparse data of liquid-side mass transfer coefficients obtained under different liquid and gas superficial velocities and systems were collected from literature and compared with the liquid-side mass transfer coefficients for benzene calculated in this work (Figure 8). It is observed that the values of benzene mass transfer coefficients are clearly higher than the majority of the points presented except for those of Shah,[2] with which they seem to bear the same range and trend. The extremely low liquid and gas velocities used in this work appear to be the reason for the observed deviations.

The calculations of the physical properties of the reacting mixture were based on correlations taken from *Chemical Properties Handbook*,[84] *Perry's Chemical Engineers' Handbook*,[85] and the book *The Properties of Gases and Liquids*[86] for multicomponent hydrocarbon gas systems at high pressures.

5.3. Downflow Versus Upflow. A comparison of the performance of the laboratory reactor in upflow and downflow modes is presented in Figure 9. The comparison is attempted at 80 °C. It is shown that, for low gas flow rates, the performance in the downflow mode of operation is superior to that of the upflow one. As the gas velocity increases, the differences decrease and the performance of the catalyst bed in downflow and upflow modes becomes identical for high gas flow rates.[11] In connection with Figure 2, it appears that the lower mass transfer coefficients at low gas velocities account for the inferior performance of the upflow reactor for the experimental conditions of this work.

6. Conclusions

A study on the benzene hydrogenation over commercial catalyst particles in a laboratory three-phase reactor is presented. The working flow regime is the trickle one.

From the comparison of rival kinetic models and from the data and the analysis presented, four models appear to describe very well the intrinsic hydrogenation rates for the experimental conditions used to perform the experiments.

An analytical reactor simulation model incorporating reaction kinetics, liquid volatility, and solvent effects predicts the experimental data very well.

Mass transfer limitations appear to have a considerable impact on reactor performance. Overall, gas-side and liquid-side mass transfer coefficients for hydrogen as well as for benzene transfer have been presented. No other experimental mass transfer data

were found in the literature for the gas and liquid velocity regions examined in this work.

For low gas velocities, mass transfer in upflow operation has a greater effect on the reactor performance, although at higher velocities the differences diminish. This is attributed to the lower mass transfer coefficients calculated for the upflow operation.

Acknowledgment

We would like to thank Motor-Oil Hellas Refinery for the financial support of this work.

Nomenclature

a, a_v = volumetric interfacial area (cm^2/cm^3)
A = internal area of the reactor (cm^2)
A_1 = preexponential factor for the specific reaction constant
A_2 = preexponential factor for the adsorption constant of hydrogen
A_3 = preexponential factor for the adsorption constant of benzene
A_0 = preexponential factor (Arrhenius law)
a_s = external area of particles and wall per unit reactor volume (cm^2/cm^3)
C_I = concentration of component I (concentration units, e.g., mol/cm^3)
C^*_{iG} = concentration of component i in the gas side of the gas−liquid interface (mol/cm^3)
C^*_{iL} = concentration of component i in the liquid side of the gas−liquid interface (mol/cm^3)
C_{LI} = concentration of component I in the liquid phase (mol/cm^3)
d_c = column diameter (cm)
D_{Gi} = diffusion coefficient of component i in the gas phase (cm^2/s)
d_K = Krischer and Kast hydraulic diameter
D_{Li} = diffusion coefficient of component i in the liquid phase (cm^2/s)
d_p = grain equivalent diameter, diameter of sphere having same volume as grain (cm)
D_α = α-phase diffusion coefficient (cm^2/s)
E_a = apparent activation energy of benzene hydrogenation (kJ/mol)
Ga = Galileo number
H_I = Henry's constant of component I
k = reaction-specific constant (depends on the units of the reaction rate)
k_i = kinetic constants (depends on the units of the reaction rate)
k_{Gi} = gas-side mass transfer coefficient of component i (s^{-1})
k_{GLi} = overall mass transfer coefficient of component i (s^{-1})
K_I = adsorption constant of component I (units of reverse concentration, e.g., cm^3/mol)
k_{Li} = liquid-side mass transfer coefficient of component i (s^{-1})
N_B = mole fraction of benzene
N_{exp} = number of experiments conducted
N_{GLi} = gas−liquid mass transfer flux of component i (mol/h)
N_{Li} = molar feed of component i in the liquid phase (mol/h)
N_{Vi} = molar feed of component i in the vapor phase (mol/h)
P_I = partial pressure of component I (pressure units, e.g., bar)
R = gas constant ($R = 8.314\,39 \pm 0.000\,34$ (abs Joule)/(deg mol))
Re_α = α-phase Reynolds number
r_p = reaction rate ($mol/h/g_{cat}$)
Sc_α = α-phase Schmidt number
T = temperature (K)
U_α = superficial α-phase velocity (cm/s)
We_α = α-phase Weber number
X_G = Lockhart−Martinelli number
X_i = experimental conversion percent of benzene hydrogenation for experiment i
$\hat{X}_i$ = predicted conversion percent of benzene hydrogenation for experiment i
z = reactor length (cm)

Greek Letters

ΔH_B = adsorption enthalpy of benzene (J/mol)
ΔH_{H_2} = adsorption enthalpy of hydrogen (J/mol)
ϵ = bed void fraction
ρ_{bed} = catalytic bed density (g/cm^3)
Φ_{min} = minimized objective function

Subscripts

α = gas or liquid
aver = average value
G or g = gas
I or i = benzene, hydrogen, cyclohexane, or *n*-hexane
L or l = liquid
V = vapor

Literature Cited

(1) Satterfield, C. N. Trickle bed reactors. *AIChE J*. **1975**, *21*, 209.
(2) Shah, T. Y. *Gas−liquid−solid reactor design*; Mc-Graw Hill: New York, 1979.
(3) Herskowitz, M.; Smith, M. J. Trickle bed reactors: A review. *AIChE J*. **1983**, 29.
(4) Ramachandran, P. V.; Chaudhari, R. V. *Three-phase catalytic reactors*; Gordon and Breach: New York, 1983.
(5) Ng, K. M.; Chu, C. F. Trickle-bed reactors. *Chem. Eng. Prog*. **1987**, *83*, 55.
(6) Gianetto, A.; Specchia, V. Trickle-bed reactors: State of art and perspectives. *Chem. Eng. Sci*. **1992**, *47*, 3197.
(7) Saroha, A. K.; Nigam, K. D. P. Trickle bed reactors. *Rev. Chem. Eng.* **1996**, *12*, 207.
(8) Al-Dahhan, M. H.; Larachi, F.; Dudukovic, M. P.; Laurent, A. High-pressure trickle-bed reactors: A review. *Ind. Eng. Chem. Res*. **1997**, *36*, 3292.
(9) Dudukovic, M. P.; Larachi, F.; Mills, P. L. Multiphase reactors−revisited. *Chem. Eng. Sci*. **1999**, *54* (21), 1975.
(10) Nigam, K. D. P.; Larachi, F. Process intensification in trickle-bed reactors. *Chem. Eng. Sci*. **2005**, *60* (22), 5880.
(11) Cheng, Z.-M.; Yuan, W.-K. Influence of hydrodynamics parameters on performance of a multiphase fixed-bed reactor under phase transition. *Chem. Eng. Sci*. **2002**, *57*, 3407.
(12) Ng, K. M. A model for flow regime transitions in cocurrent downflow trickle-bed reactors. *AIChE J*. **1986**, *32*, 115.
(13) Holub, R. A.; Dudukovic, M. P.; Ramachandran, P. A. Pressure drop, liquid holdup and flow regime transition in trickle flow. *AIChE J*. **1993**, *39*, 302.
(14) Fukushima, S.; Kusaka, K. Interfacial area and boundary of hydrodynamic flow region in packed column with cocurrent downward flow. *J. Chem. Eng. Jpn.* **1977**, *10*, 461.
(15) Fukushima, S.; Kusaka, K. Liquid-phase volumetric and mass-transfer coefficient, and boundary of hydrodynamic flow region in packed column with cocurrent downward flow. *J. Chem. Eng. Jpn.* **1977**, *10*, 468.
(16) Charpentier, J. C. Recent progress in two-phase gas−liquid mass transfer in packed beds. *Chem. Eng. J*. **1976**, *11*, 161.
(17) Tsamatsoulis, C. D.; Papayannakos, G. N. Partial Wetting of Cylindrical Catalytic Carriers in Trickle-Bed Reactors. *AIChE J*. **1996**, *42*, 7.
(18) Pironti, F.; Mizrahi, D.; Acosta, A.; Gonzalez-Mendizabal, D. Liquid−solid wetting factor in trickle-bed reactors: Its determination by a physical method. *Chem. Eng. Sci.* **1999**, *54*, 3793.
(19) Kundu, A.; Nigam, K. D. P.; Verma, R. P. Catalyst wetting characteristics in trickle-bed reactors. *AIChE J*. **2003**, *49* (9), 2253.
(20) Ruecker, M. C.; Akgerman, A. Determination of wetting efficiencies for a trickle-bed reactor at high temperatures and pressures. *Ind. Eng. Chem. Res*. **1987**, *26*, 164.
(21) Levec, J.; Lakota, A. Solid−liquid mass transfer in packed beds with cocurrent downward two-phase flow. *AIChE J*. **1990**, *36*, 9, 1444.

(22) Burghardt, A.; Kolodziej, A.; Jaroszynski, M. Experimental studies of liquid−solid wetting efficiency in trickle-bed cocurrent reactors. *Chem. Eng. Process.* **1990** *28*, 35.

(23) Funk, G. A.; Harold, M. P.; Ng, K. M. Experimental study of reaction in a partially wetted catalytic pellet. *AIChE J.* **1991**, *37* (2), 202.

(24) Llano, J.; Rosal, R.; Sastre, H.; Diez, F. V. Determination of wetting efficiency in trickle-bed reactors by a reaction method. *Ind. Eng. Chem. Res*. **1997**, *36*, 2616.

(25) Gonzalez-Mendizabal, D.; Aguilera, M. E.; Pironti, F. Solid−liquid mass transfer and wetting factors in trickle bed reactors: Effect of the type of solid phase and the presence of chemical reaction. *Chem. Eng. Commun.* **1998**, *169*, 37.

(26) Mills, P. L.; Dudukovic, M. P. Analysis of catalyst effectiveness in trickle-bed reactors processing volatile or nonvolatile reactants. *Chem. Eng. Sci*. **1980**, *35*, 2267.

(27) Herskowitz, M. Wetting efficiency in trickle-bed reactors. The overall effectiveness factor of partially wetted catalyst particles. *Chem. Eng. Sci*. **1981**, *36* (10), 1665.

(28) Tan, C.-S. Effectiveness factors of *n*-th order reactions for incomplete wetting particles in trickle-bed reactors. *Chem. Eng. Sci*. **1988**, *43* (6), 1281.

(29) Ring, Z. E.; Missen, R. W. Trickle-bed reactors: An experimental study of partial wetting effect. *AIChE J.* **1989**, *35* (11), 1821.

(30) Iliuta, I.; Larachi, F. The generalized slit model: Pressure gradient, liquid holdup, & wetting efficiency in gas−liquid trickle flow. *Chem. Eng. Sci*. **1999**, *54*, 5039.

(31) van Klinken, J.; van Dongen, R. H. Catalyst dilution for improved performance of laboratory trickle-flow reactors. *Chem. Eng. Sci*. **1980**, *35*, 59.

(32) Tsamatsoulis, D.; Papayannakos, N. Axial dispersion and hold-up in a bench-scale trickle-bed reactor at operating conditions. *Chem. Eng. Sci*. **1994**, *49*, 4.

(33) Al-Dahhan, M. H.; Dudukovic, M. P. Catalyst bed dilution for improving catalyst wetting in laboratory trickle-bed reactors. *AIChE J*. **1996**, *42* (9), 2594.

(34) Wammes, W. J. A.; Middelkamp, J.; deBaas, C. M.; Westerterp, K. R. Hydrodynamics in a cocurrent gas−liquid trickle bed at elevated pressures. *AIChE J*. **1991**, *37* (12), 1849.

(35) Al-Dahhan, M. H.; Dudukovic, M. P. Catalyst wetting efficiency in trickle-bed reactors at high pressure. *Chem. Eng. Sci*. **1995**, *50* (15), 2377.

(36) Burghardt, A.; Bartelmus, G.; Jaroszynski, M.; Kolodziej, A. Hydrodynamics and mass transfer in a three-phase fixed-bed reactor with cocurrent gas−liquid downflow. *Chem. Eng. J.* **1995**, *58*, 83.

(37) Stuber, F.; Wilhelm, A. M.; Delmas, H. Modeling of three-phase catalytic upflow reactor: A significant chemical determination of liquid−solid and gas−liquid mass transfer coefficients. *Chem. Eng. Sci*. **1996**, *51* (10), 2161.

(38) Thanos, A. Non ideal flow of upflow pilot hydrotreaters. Ph.D. Thesis, National Technical University of Athens (NTUA), Athens, Greece, 1997.

(39) Colombo, A. J.; Baldi, G.; Sicardi, S. Solid−liquid contacting effectiveness in trickle bed reactors. *Chem. Eng. Sci*. **1976**, *31*, 1101.

(40) Turek, F.; Lange, R. Mass transfer in trickle-bed reactors at low Reynolds number. *Chem. Eng. Sci*. **1981**, *36*, 569.

(41) Morsi, B. I.; Laurent, A.; Midoux, N.; Barthole-Delaunay, N.; Storck, A.; Charpentier, J. C. Hydrodynamics and gas−liquid−solid interfacial parameters of co-current downward two-phase flow in trickle-bed reactors. *Chem. Eng. Commun*. **1984**, *25*, 267.

(42) Yaichi, W.; Laurent, A.; Midoux, N.; Charpentier, J. C. Determination of gas-side mass transfer coefficients in trickle-bed reactors in the presence of an aqueous or an organic liquid phase. *Int. Chem. Eng.* **1988**, *28*, 299.

(43) Wild, G.; Larachi, F.; Charpentier, J. C. Heat and mass transfer in gas−liquid−solid fixed bed reactors. In *Heat and Mass Transfer in Porous Media*; Quintard, M., Todorovic, M.; Elsevier: Amsterdam, The Netherlands, 1992.

(44) Iliuta, I.; Larachi, F.; Grandjean, B. P. A.; Wild, G. Gas−liquid interfacial mass transfer in trickle-bed reactors: State-of-the-art correlations. *Chem. Eng. Sci*. **1999**, *54*, 5639.

(45) Larachi, F.; Belfares, L.; Iliuta, I.; Grandjean, P. A. Heat and mass transfer in cocurrent gas−liquid packed beds. Analysis, recommendations, and new correlations. *Ind. Eng. Chem. Res.* **2003**, *42*, 222.

(46) Goto, S.; Smith, J. M. Trickle-bed reactor performance. Part I. Holdup and mass transfer effects. *AIChE J.* **1975**, *21*, 706.

(47) Martin, J. M.; Combarnous, M.; Charpentier, J. C. Physical gas−liquid mass transfer for co-current flow through porous medium with low liquid and gas flowrates corresponding to the conditions of enhanced oil recovery. *Chem. Eng. Sci*. **1980**, *35*, 2362.

(48) Samb, F. M.; Deront, M.; Adler, N.; Peringer, P. Dynamic liquid holdup and oxygen mass transfer in a cocurrent upflow bioreactor with small packing as low Reynolds number. *Chem. Eng. J*. **1996**, *62*, 237.

(49) Lara Marquez, A.; Larachi, F.; Wild, G.; Laurent, A. Mass transfer characteristics of fixed beds with cocurrent upflow and downflow. *Chem. Eng. Sci*. **1992**, *47* (13/14), 3485.

(50) Larachi, F.; Cassanello, M.; Laurent, A. Gas−liquid interfacial mass transfer in trickle-bed reactors at elevated pressures. *Ind. Eng. Chem. Res*. **1998**, *37*, 718.

(51) Midoux, N.; Morsi, B. I.; Purwasasmita, M.; Laurent, A.; Charpentier, J. C. Interfacial area and liquid side mass transfer coefficient in trickle bed reactors operating with organic liquids. *Chem. Eng. Sci*. **1984**, *39* (5), 781.

(52) Goenaga, A.; Smith, J. M.; McCoy, B. J. Study of gas-to-liquid mass transfer by dynamic methods in trickle beds. *AIChE J*. **1989**, *35* (1), 159.

(53) Toppinen, S.; Aittamaa, J.; Salmi, T. Interfacial mass transfer in trickle-bed reactor modeling. *Chem. Eng. Sci*. **1996**, *51* (18), 4335.

(54) Iliuta, I.; Thyrion, F. C. Gas−liquid mass transfer in fixed beds with two-phase cocurrent downflow: Gas/Newtonian and non-Newtonian liquid systems. *Chem. Eng. Technol*. **1997**, *20*, 538.

(55) Evren, V.; Özdural, A. R. A new technique for the determination of mass transfer coefficients in packed columns for physical gas absorption systems. *Chem. Eng. J*. **1995**, *57*, 67.

(56) Benadda, B.; Kafoufi, K.; Monkam, P.; Otterbein, M. Hydrodynamics and mass transfer phenomena in counter-current packed column at elevated pressures. *Chem. Eng. Sci*. **2000**, *55*, 6251.

(57) Bin, A. K.; Duczmal, B.; Machniewski, P. Hydrodynamics and ozone mass transfer in a tall bubble column. *Chem. Eng. Sci*. **2001**, *56*, 6233.

(58) Dluska, E.; Wronski, S.; Hubacz, R. Mass transfer in gas−liquid Couette−Taylor flow reactor. *Chem. Eng. Sci*. **2001**, *56*, 1131.

(59) Satterfield, C. N.; Ozel, F. Direct solid-catalyzed reaction of a vapor in an apparently completely wetted trickle bed reactor. *AIChE J*. **1973**, *19* (6), 1259.

(60) Sharma, D. S.; Gadgil, K.; Sarkar, K. M. Estimation of Kinetic Parameters of Benzene Hydrogenation in a Trickle Bed Reactor. *Chem. Eng. Technol*. **1993**, *16*, 347.

(61) Chou, P.; Vannice, M. A. Benzene hydrogenation over supported and unsupported palladium. II. Reaction model. *J. Catal.* **1987**, *107*, 140.

(62) Zrncevic, S.; Rusic, D. Verification of the kinetic model for benzene hydrogenation by poisoning experiment. *Chem. Eng. Sci*. **1988**, *43* (4), 763.

(63) Coughlan, B.; Keane, M. A. The Hydrogenation of Benzene over Nickel Supported Y Zeolites. Part 1. A Kinetic Approach. *Zeolites* **1991**, *11*, 12.

(64) Lin, S. D.; Vannice, M. A. Hydrogenation of Aromatic Hydrocarbons over Supported Pt Catalysts. I. Benzene Hydrogenation. *J. Catal*. **1993**, *143*, 539.

(65) Stanislaus, A.; Cooper, B. Aromatic Hydrogenation Catalysis: Review. *Catal. Rev.—Sci. Eng*. **1994**, *36*, 75.

(66) Smeds, S.; Murzin, D.; Salmi, T. Kinetics of Ethylbenzene Hydrogenation on Ni/Al_2O_3 *Appl. Catal., A* **1995**, *125*, 271.

(67) Keane, M. A.; Patterson, M. P. The Role of Hydrogen Partial Pressure in the Gas-Phase Hydrogenation of Aromatics over Supported Nickel. *Ind. Eng. Chem. Res*. **1999**, *38*, 1295.

(68) Louloudi, A.; Michalopoulos, J.; Gangas, N.-H.; Papayannakos N. Hydrogenation of benzene on Ni/Al-pillared saponite catalysts. *Appl. Catal. A* **2003**, *242*, 41.

(69) Saeys, M.; Thybaut W. J.; Neurock M.; Marin B. G. Kinetic models for catalytic reactions from first principles: Benzene hydrogenation. *Mol. Phys.* **2004**, *102* (3), 267.

(70) Murzin, Yu. D.; Sokolova, A. N.; Kul'kova, V. N.; Temkin, I. M. Kinetics on Liquid-Phase Hydrogenation of Benzene and Toluene on a Nickel Catalyst. *Kinet. Katal*. **1989**, *30* (6), 1352.

(71) Toppinen, S. Rantakylä, T. K.; Salmi, T.; Aittamaa, J. Kinetics of the Liquid-Phase Hydrogenation of Benzene and Some Monosubstituted Alkylbenzenes over a Nickel Catalyst. *Ind. Eng. Chem. Res*. **1996**, *35*, 1824.

(72) Singh, U. K.; Vannice, M. A. Kinetic and Thermodynamic Analysis of Liquid-Phase Benzene Hydogenation. *AIChE J*. **1999**, *45* (5), 1059.

(73) Franco, J.; Marzuka, S.; Papa, J.; de Herrera, J. T. Kinetic parameters evaluation for the catalytic hydrogenation of benzene, toluene and ethyl-benzene. *Recents Prog. Genie Proc.* **1999**, *13* (65), 123.

(74) Rantakylä, T. K.; Toppinen, S.; Salmi, T.; Aittamaa, J. Investigation of the Hydrogenation of Some Substituted Alkylbenzenes in a Laboratory Scale Trickle-Bed Reactor. *J. Chem. Technol. Biotechnol*. **1996**, *67*, 265.

(75) Murzin, D. Yu.; Kul'kova, N. V. Nonequilibrium effects in the liquid-phase catalytic hydrogenation. *Catal. Today* **1995**, *24*, 35.

(76) Rautanen, P. A.; Aittamaa, J. R.; Krause, A. O. Solvent effect in liquid-phase hydrogenation of toluene. *Ind. Eng. Chem. Res.* **2000**, *39*, 4032.

(77) Rao, S. S. *Optimization Theory and Applications*, 2nd ed.; Wiley Eastern Limited: New Delhi, India, 1984.

(78) Hairer, E.; Norsett, P. S.; Wanner, G. *Solving ordinary differential equations I: nonstiff problems*; Springer-Verlag: Berlin, 1993.

(79) Graboski, M. S.; Daubert, T. E. A Modified Soave Equation of State for Phase Equilibrium Calculations. 1. Hydrocarbon Systems. *Ind. Eng. Chem. Process Des. Dev.* **1978**, *17*, 443.

(80) Agarwal, A. K.; Brisk, M. L. Sequential experimental design for precise parameter estimation. 1. Use of reparameterization. *Ind. Eng. Chem. Process Des. Dev.* **1985**, *24*, 203.

(81) Kittrell, R. J.; Mezaki, R.; Watson, C. C. Estimation of parameters for nonlinear least squares analysis. *Ind. Eng. Chem.* **1965**, *57* (12), 18.

(82) Lindfords, P. L.; Salmi, T. Kinetics of toluene hydrogenation on a supported Ni catalyst. *Ind. Eng. Chem. Res.* **1993**, *32*, 34.

(83) Ellman, M. J.; Midoux, N.; Laurent, A.; Charpentier, J. C. A new improved pressure drop correlation for trickle-bed reactors. *Chem. Eng. Sci.* **1988**, *43*, 2201.

(84) *Chemical Properties Handbook*. 7th ed.; McGraw-Hill: New York, 1999.

(85) *Perry's Chemical Engineers' Handbook*, 7th ed.; McGraw-Hill: New York, 1999.

(86) Reid, R. C.; Prausnitz, J. M.; Poling, B. E. *The Properties of Gases and Liquids*; McGraw-Hill: New York, 1987.

Received for review May 9, 2006
Revised manuscript received August 2, 2006
Accepted August 16, 2006

IE060577A